Derivation and Evaluation of the Advanced Corner Modeling Method

By Martin J King
MJKing57@aol.com

July 03, 2024

Table of Contents

Introduction

The long axial lengths required in TL designs almost always results in a folding of the path to make it fit within a conventional rectangular shaped enclosure. The behavior of folded geometries used in TL enclosures has almost as many rules of thumb and postulated acoustic behaviors as the fiber stuffing did before modern measurement and TL simulation software became available. There are many proposals for how to accurately model the convoluted acoustic path as it navigates through a series of folds/bends and what to assume as section lengths and cross-sectional areas.

After reviewing the correlation between measured and simulated results from my recent Satori TL design and build (see first reference), one of the areas identified for subsequent study was the behavior and impact of the single 180-degree fold at the top of the enclosure and the final 90-degree bend at the bottom just before the rear terminus. I believe that the outcome of this study generated an accurate method for modeling these geometric discontinuities. A more detailed description of this Advanced Corner Modeling Method and some demonstrative results will be presented in the following slides

Current Methods Used by DIYers to Represent a Fold in a TL or Horn Geometry

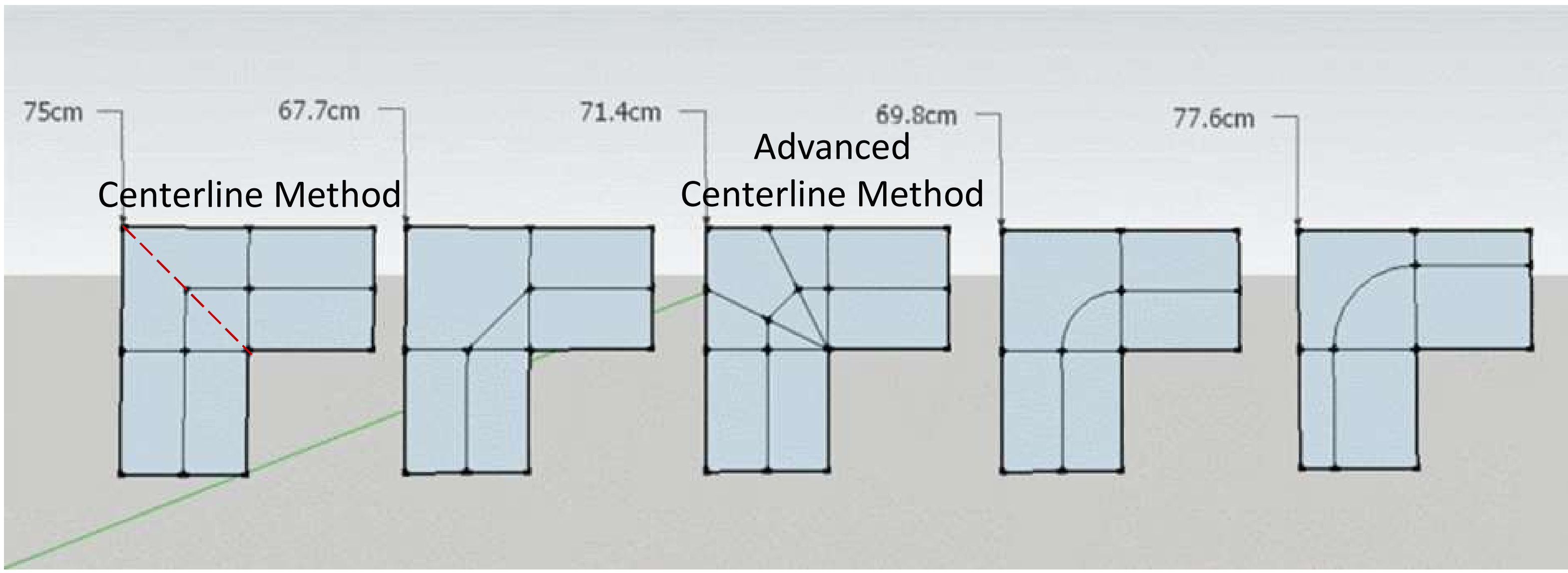

I lifted this picture from the Internet. I do not know its origin, but it is referenced on many on-line forums and discussion groups. In the past when I modeled a TL, I used the left-hand method, the Centerline Method, with the addition of a diagonal (red dashed line) across the corner. Hornresp users tend to favor the middle modeling method, the Advanced Centerline Method.

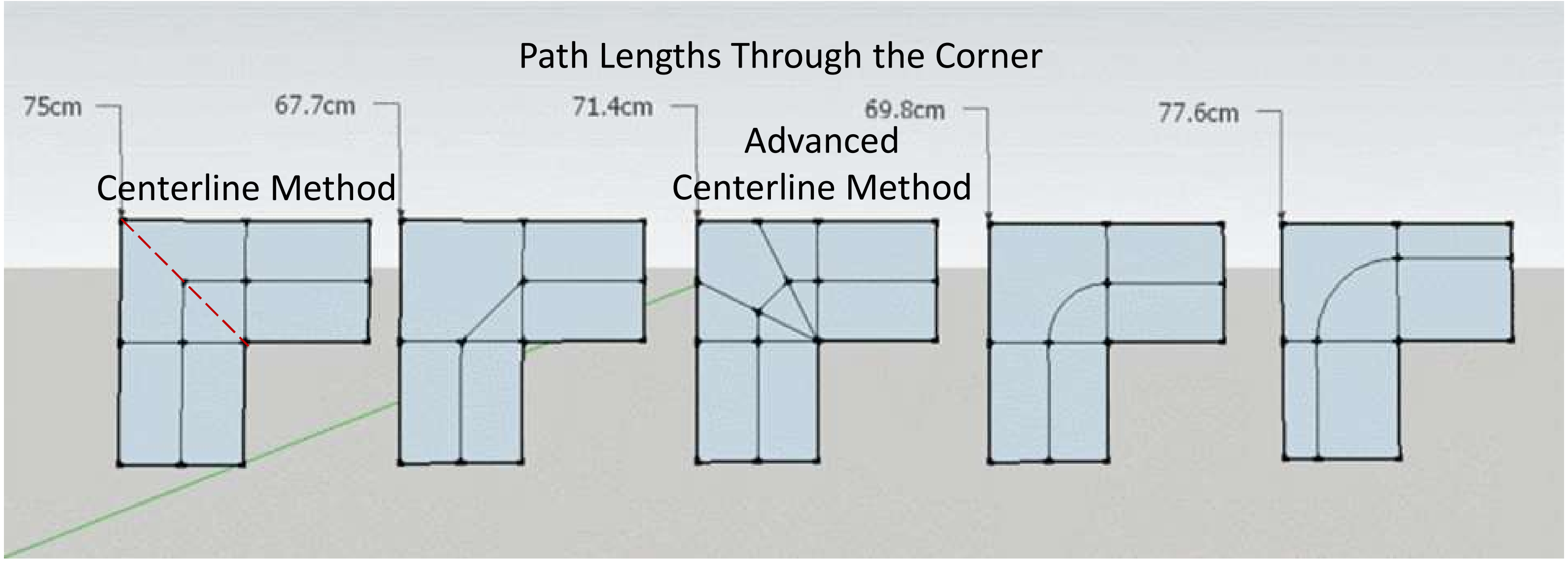

The primary difference in these five methods for modeling corners is the effective path length, as shown in the figure, which has a maximum of 77.6 cm and a minimum of 67.7 cm.

Anecdotal observations from many builders of folded TL's are that the tuning frequency is higher than predicted using the Centerline Method and that the folds act as a low pass filter attenuating the higher harmonics. Changing the corner modeling method is typically used to adjust the effective TL length resulting in an improved correlation with the measured frequencies, but the low pass filtering effect is not predicted by any of these corner modeling methods.

There are several assumptions that go along with these methods of modeling the folds/bends using 1-dimensional acoustic elements.

- Each section of the bend geometry is represented by a 1-dimensional acoustic element that has a length and a cross-sectional area defined at each end.
- At each cross-sectional area, the pressure and volume velocity are assumed to be constant. Also, the pressure and volume velocity are continuous between elements.
- Each acoustic element contains equations that relate the pressure and volume velocity at the first cross-sectional area to the second cross-sectional area using a transfer matrix [T].
- Almost all 1-dimensional simulation codes analyze a series of acoustic elements placed along the length of the TL. The programs see this chain of elements as lying on a straight line, the impact of an actual geometric change in direction is not explicitly modeled.

The most popular 1-dimensional simulation codes including HornResp, Leonard Audio's TL code, SPICYTL, as well as my own MathCad worksheets all work the same way. Augspurger's TL code uses a discretized equivalent circuit analysis, but it has similar assumptions

Discussion and Derivation of the Advanced Corner Modeling Method

To simplify the analysis and eliminate all other contributing variables to a sample TL's acoustic response, the following assumptions were made.

- The TL geometry has a constant cross-sectional area with one 180-degree fold at the top of the enclosure and a 90-degree bend at the bottom rear terminus end of the enclosure.
- The driver was placed at the closed end of the TL to maximize the excitation of all quarter-wavelength standing waves.
- The acoustic impedance at the open end was set to the simple zero pressure and zero derivative of velocity boundary conditions, no frequency dependent damping was present in this impedance.
- A very small amount of distributed damping was applied to the air volume in the TL to prevent the response going to infinity at the standing wave frequencies.

These assumed conditions allow the study to focus only on the vibrating air column formed by the TL enclosure. This also allows a direct comparison between a closed form solution, MathCad calculated results, and an ANSYS finite element model's plotted results.

The TL enclosure being studied has a length of 103 inches (2.616 m) for a tuning frequency of ~33 Hz and a constant cross-sectional area of 59.288 square inches (382.5 cm^2). These dimensions are driven by a Satori WO25P-4 woofer's Thiele/Small parameters.

To double check the modeling methods, the TL geometry is assumed to be straight and have a uniform cross-sectional area. The calculated model results are compared with the closed form quarter-wave frequencies.

$$f_{closed\ form} = n/4 \times (c / L) \quad \text{where } n = 1,3,5,\ldots.$$

Mode	Closed Form	MathCad Straight	ANSYS Straight
1/4	32.87	32.60	33.08
3/4	98.62	97.95	99.24
5/4	164.36	163.45	165.41
7/4	230.10	228.80	231.60
9/4	295.85	294.25	297.82
11/4	361.59	359.60	364.07
13/4	427.34	425.05	430.35
-	[Hz]	[Hz]	[Hz]

The MathCad and ANSYS predicted frequencies are all withing 1% of the calculated closed form solution, the three different modeling methods check.

MathCad 1D Folded Model

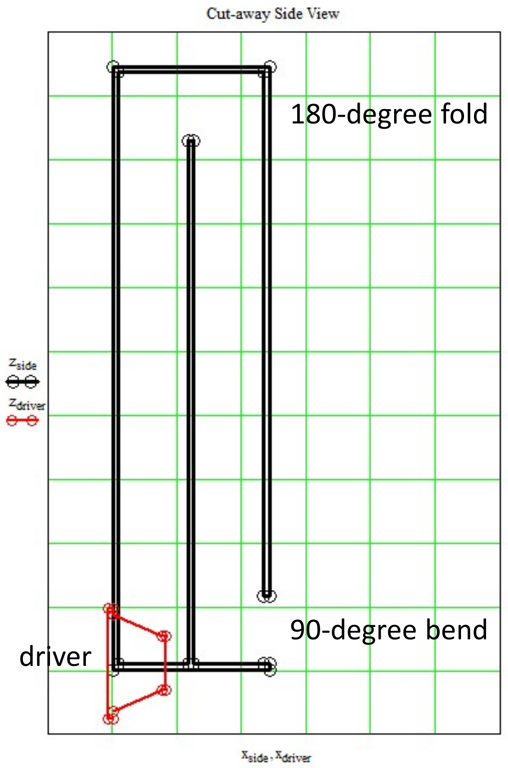

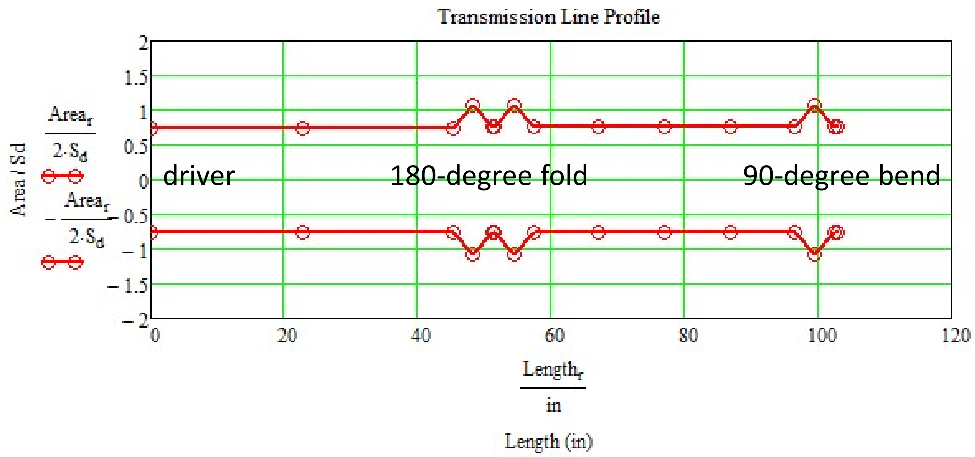

On the left is the MathCad geometry schematic of the folded TL with the driver placed at the closed end. Above is the path and cross-sectional area layout using the Centerline Method for modeling the 180-degree fold and 90-deg bend. The acoustic model is a straight path even though the actual geometry is folded. The peaks in the MathCad calculated acoustic impedance frequency response plot correspond to the TL's quarter-wavelength standing waves.

ANSYS 3D Folded Model

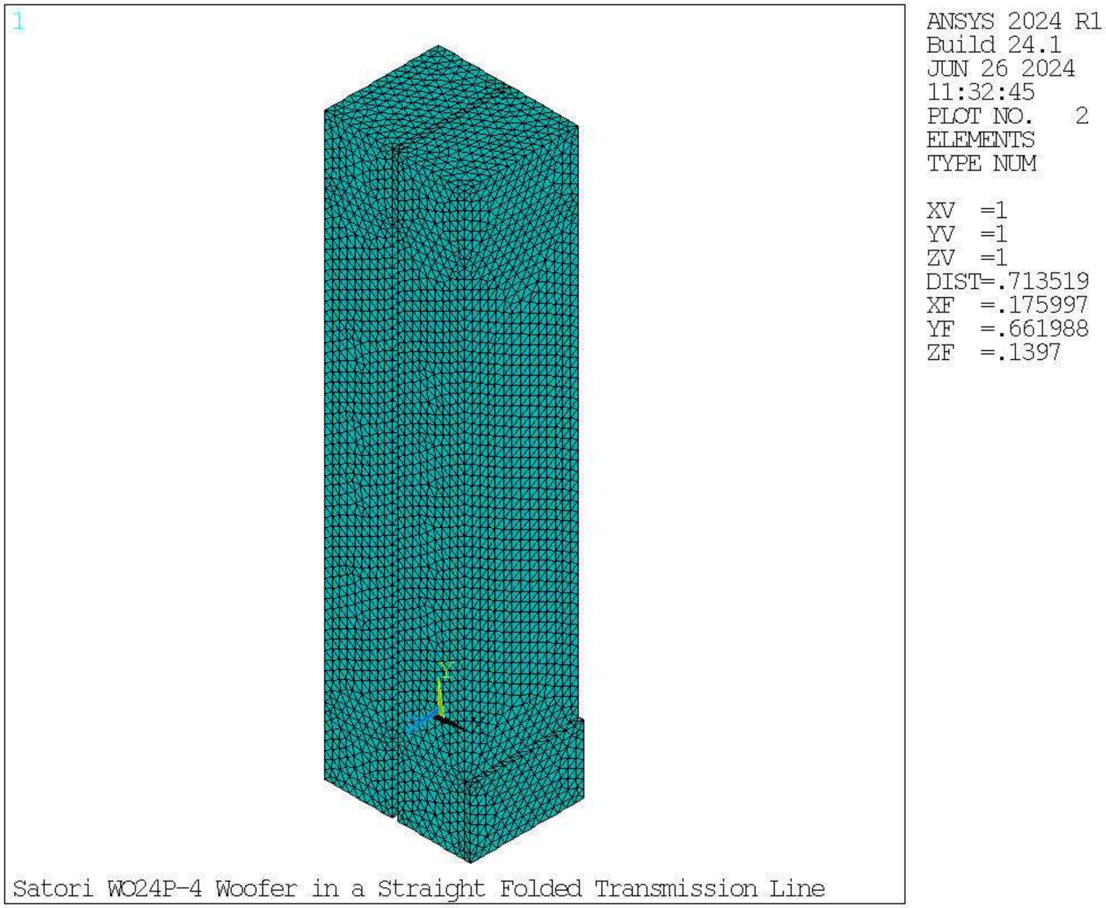

On the left is the ANSYS 3D finite element model of the air volume in the folded TL. The dimensions and properties of the air volume are identical to the MathCad model shown in the previous slide.

The advantage of the ANSYS finite element model is that the pressure profile is calculated for each quarter-wavelength standing wave in 3D, it is not limited to a straight 1D path. No assumptions are made about the profile or distribution of the pressure across any cross-section.

The first seven standing eaves for the 3D volume are included in Attachment 1. The frequencies and the 3D pressure profile are the correct physics result for this geometry.

The comparison table shown on slide 8 was updated to show the results for the two folded models. Again, the MathCad results are for the Centerline Method of corner modeling as shown in the figure on slide 5, the left most method.

The closed form and the MathCad Centerline Method calculated frequencies correlate within 1%. The differences between MathCad and ANSYS 3D FEM results increases to greater than 5% for some modes, not good.

$$f_{closed\ form} = n/4\ (c\ /\ L) \quad \text{where } n = 1,3,5,....$$

Mode	Closed Form	MathCad Centerline	ANSYS Folded
1/4	32.87	32.75	34.90
3/4	98.62	98.50	104.12
5/4	164.36	164.45	175.02
7/4	230.10	229.90	241.42
9/4	295.85	295.45	314.13
11/4	361.59	360.50	376.52
13/4	427.34	425.15	447.21
-	[Hz]	[Hz]	[Hz]

The MathCad and ANSYS correlation could be improved by going to the Advanced Centerline Method, but this is more of a fudging of the length and not really a physics-based modeling method.

To improve the MathCad modeling of the TL's corners, the ANSYS normalized pressure results were replotted for just the 180-degree fold region.

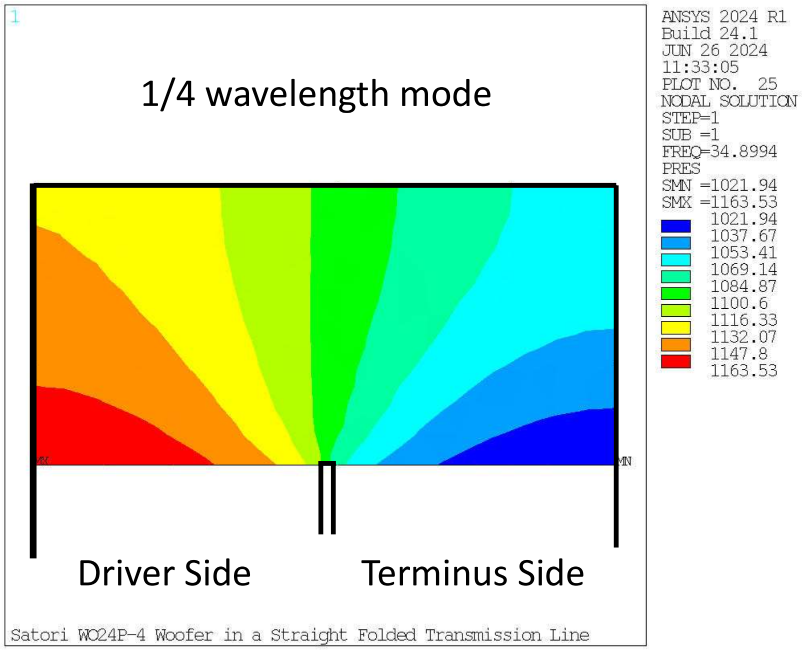

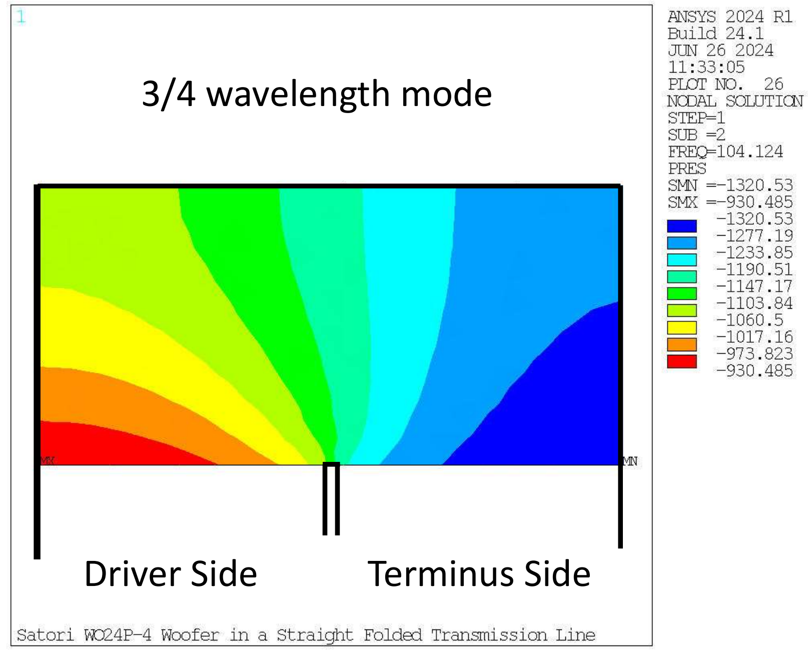

Above are the pressure profiles for the first two standing waves, notice the fan shaped pressure distribution with the contours being closer along the inside path and spreading as you move towards the outside path of the 180-degree fold. Thinking about these two plots and the 1D wave equation generated the insights used for improving the MathCad corner modeling.

Newton's 2^{nd} Law : Summation of Forces = Mass x Acceleration

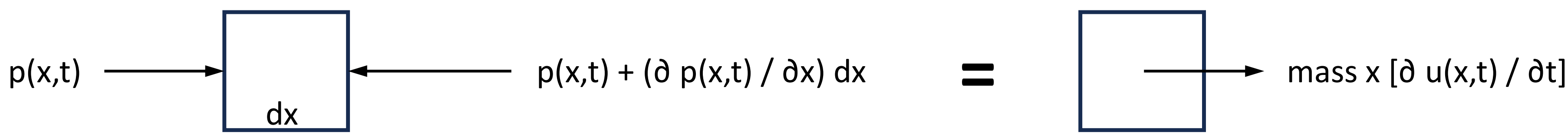

where mass = $\rho\, dx\, dy\, dz$ and $a(x,t) = \partial u(x,t) / \partial t$

$$[p(x,t) - (p(x,t) + (\partial p(x,t) / \partial x)\, dx)]\, dy\, dz = \rho\, dx\, dy\, dz\, (\partial u(x,t) / \partial t)$$

$$- \partial p(x,t) / \partial x = \rho\, (\partial u(x,t) / \partial t)$$

$$\boxed{- \partial p(x) / \partial x = j\, \omega\, \rho\, u(x)}$$

This final equation indicates that the rate of change of pressure with distance (the slope of the axial pressure profile) determines the velocity of the air, increasing pressure pushes air back in the opposite direction. Stating it another way, increasing pressure with distance produces a net force directed towards the left in the picture above resulting in an acceleration to the left. Also notice the "j" on the right side of the equation indicating a 90-degree phase difference between pressure and velocity.

$$- \partial p(x) / \partial x = j \omega \rho u(x)$$

Newton's second law is repeated above. In the equation, consider "x" to be the length variable along the centerline of the folded TL. Don't think of "x" as just the horizontal coordinate in a 3D cartesian coordinate system, "x" follows the centerline path up and down the straight regions and through the 180-degree fold and 90-degree bend. The "x" variable spans 0 inches to 103 inches as shown in the right-hand plot on slide 9.

Looking at the pressure gradients on slide 12, as they transition through the 180-degree fold you can see the fan-like pattern. The pressure contours are essentially constant across the axial path which is consistent with the assumptions of slide 6. But the gradient of the pressure decreases (larger distance between pressure contours) as you move from the inside to the outside of the 180-degree fold. The pressure gradient along the inside of the fold is much higher than the gradient along the outside of the fold. From Newtons 2^{nd} Law, this would indicate that the oscillating air velocity is not uniform when moving outward along a cross-sectional area which is inconsistent with the assumptions on slide 6. The oscillating velocity has a higher magnitude at the inside of the fold and decreases moving towards the outside of the fold.

Since the oscillating velocity must be parallel to the enclosure walls, the lines of constant pressure are normal to the exterior walls and the dividing panel. The pressure gradient going in and coming out of the fold returns to being constant across the cross-sectional area (hence velocity is also constant) and normal to the TL's axial path, this can be seen in the vertical sections of the mode shapes plotted in Attachment 1.

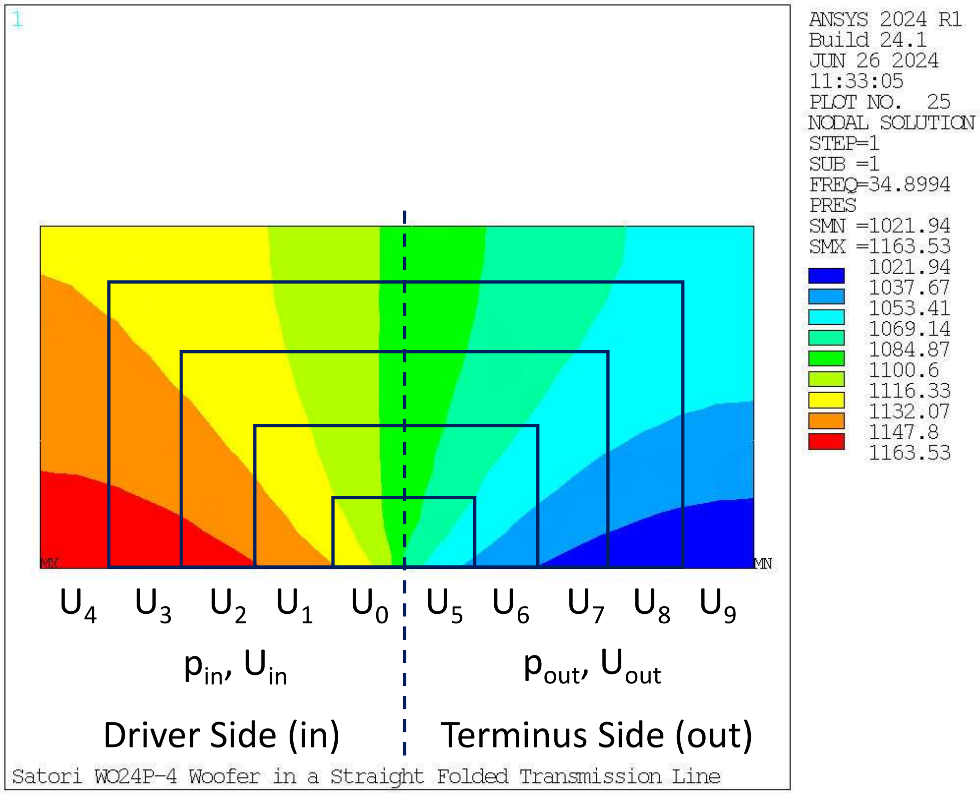

The Advanced Corner Modeling Method breaks up the fold into many parallel paths. The pressures, p_{in} and p_{out}, at the ends of the different paths on each side of the fold are assumed to be uniform while the volume velocities in the individual paths are the unknowns. The sum of the volume velocities on each side equal U_{in} and U_{out} respectively.

Solving for p_{in}, p_{out}, U_{in}, and U_{out} yields a transfer matrix that describes the acoustics of the 180-degree fold or 90-degree bend. Notice the entire air volume is now used in describing the acoustics of the corner. The programming for this method has configured with the number of parallel paths as an input variable, at left 5 paths are shown but it could just as easily be 50 paths (much harder to sketch).

Increasing the number of paths to 10, 20, 50, 100, or even 200 Increases accuracy but unfortunately also the simulation run time.

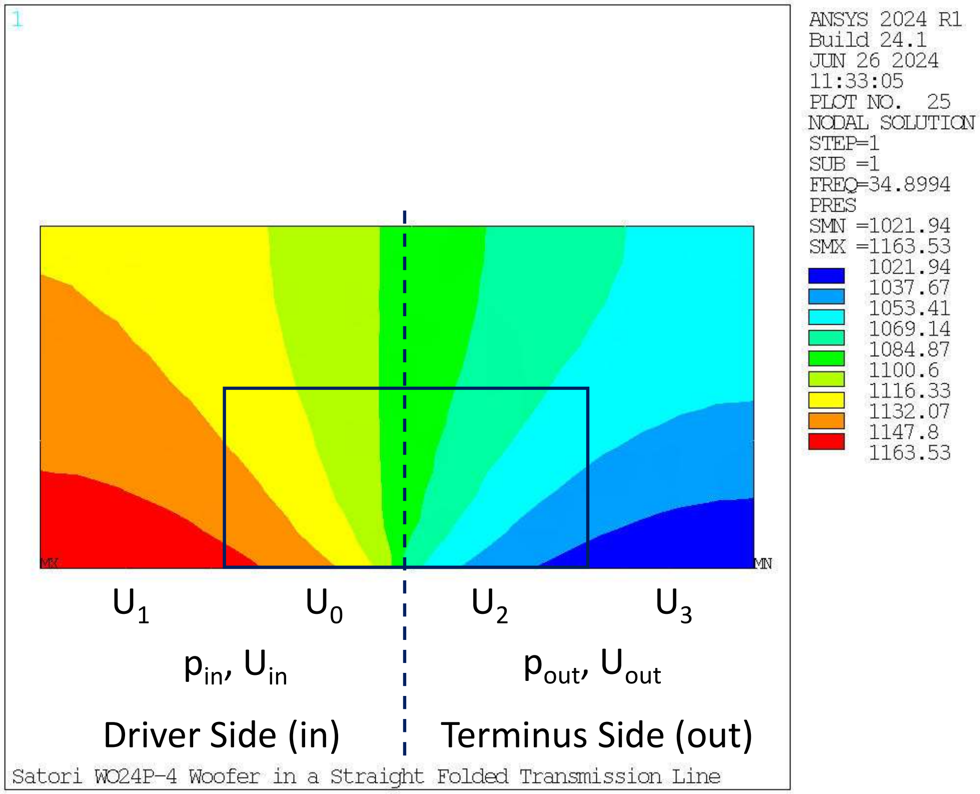

As an example, the equations for a two-path simulation of the 180-degree fold are shown below in matrix notation. The [T} matrices are transfer matrices which are functions of path length and geometry.

$[p_{in}\ U_0]^T = [T_{path\_0}] \times [p_{out}\ U_2]^T$ eq. 1 and 2

$[p_{in}\ U_1]^T = [T_{path\_1}] \times [p_{out}\ U_3]^T$ eq. 3 and 4

$U_{in} = U_0 + U_1$ and $U_{out} = U_2 + U_3$ eq. 5 and 6

There are eight unknowns (p_{in}, p_{out}, U_{in}, U_{out}, U_0, U_1, U_2, U_3) and six equations.

When calculating the acoustic impedance of a TL, the terminus impedance is specified first. Then you work your way back towards the driver end, through each section, using [T] matrices. When you reach the output of the fold, p_{out} and U_{out} are determined. This leaves six equations and six unknowns. After solving for p_{in} and U_{in}, they are used to continue the calculation to the driver end using [T] matrices.

The final result is the TL's acoustic impedance Z_{al} as seen by the driver including the Advanced Corner Modeling Method used for the 180-degree fold and the 90-degreed bend

The comparison table shown on slide 11 was updated to show the results for the Mathcad Centerline Method, MathCad Advanced Corner Modeling Method (labeled as MathCad Paths), and the ANSYS 3D folded FE model. Again, the MathCad results are for the Centerline Method of corner modeling, as shown in the figure on slide 5, and the new Advanced Corner Modeling Method shown in slide 15 but with 200 paths specified.

The MathCad Advanced Corner Modeling Method correlates very closely with the more accurate ANSYS FE results, most modes are predicted within 1%. A big improvement.

Mode	MathCad Centerline	MathCad Paths	ANSYS Folded
1/4	32.75	34.88	34.90
3/4	98.50	103.88	104.12
5/4	164.45	175.13	175.02
7/4	229.90	236.75	241.42
9/4	295.45	314.75	314.13
11/4	360.50	366.63	376.52
13/4	425.15	458.00	447.21
-	[Hz]	[Hz]	[Hz]

Plotted below are the acoustic impedance Z_{al} seen by the driver and the velocity ratio ε between the driver and the terminus output. The important difference between these two results is the low pass filter effect seen in the plots for the Advanced Corner Modeling Method. The Advanced Corner Modeling Method more accurately predicts the standing wave frequencies as well as the low pass filter effect described in slide 5.

Centerline Method

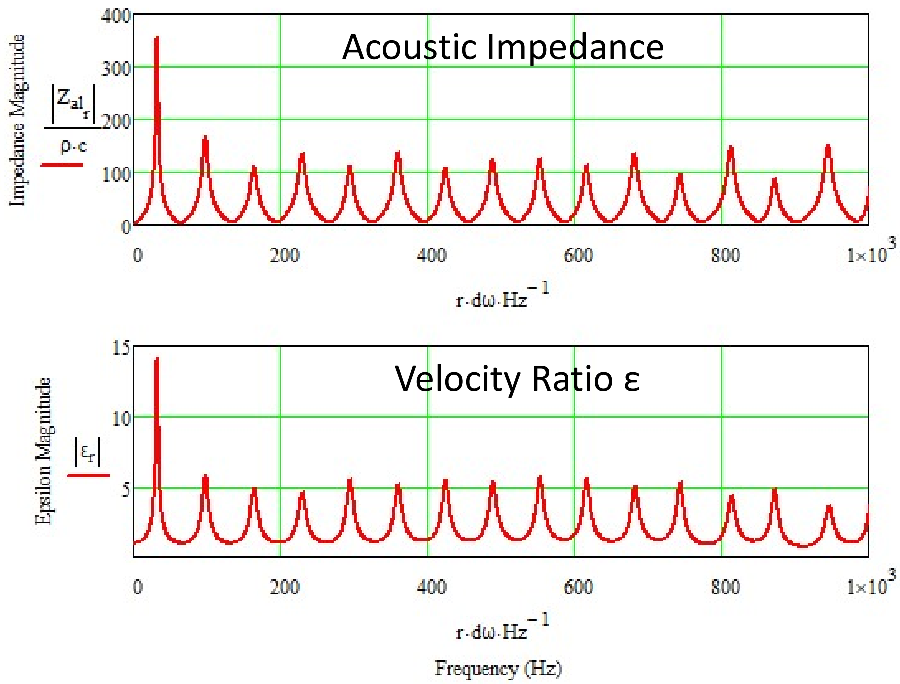

Advanced Corner Modeling Method

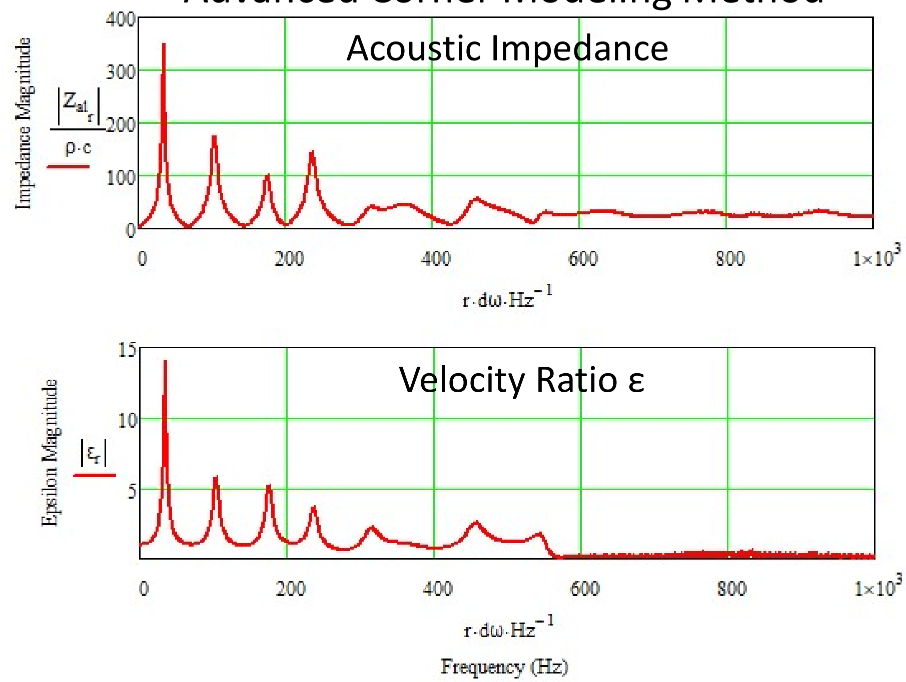

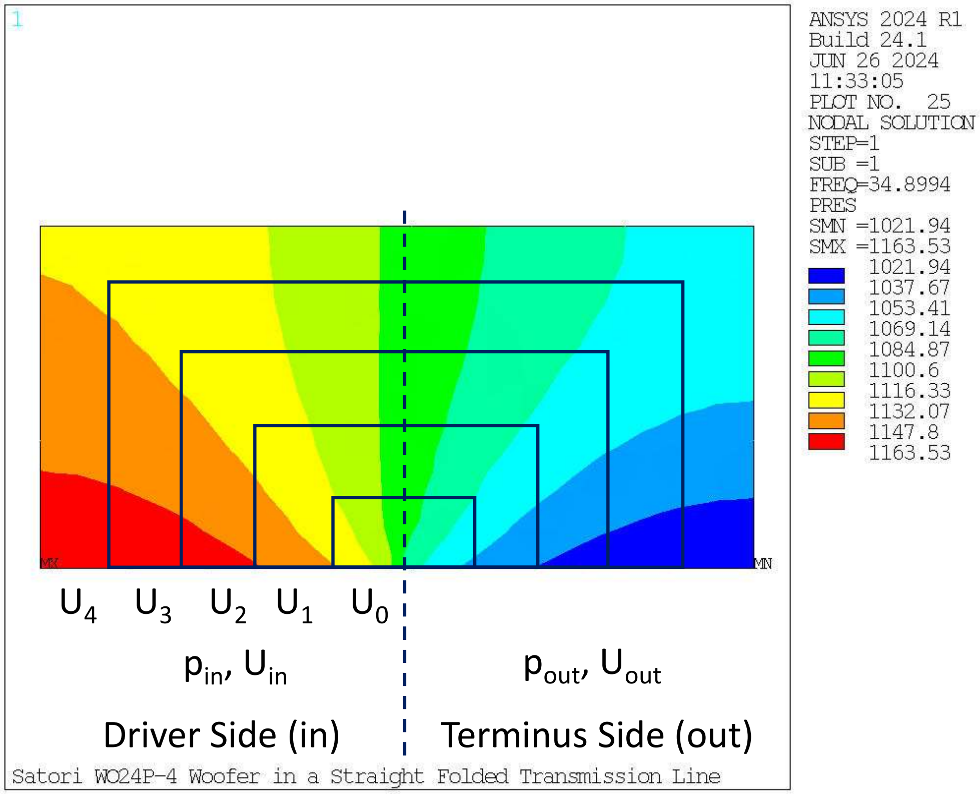

To try and explain the impact of modeling the fold as a set of parallel paths, the figure from slide 15 is modified and reproduced.

Working from the driver end of the TL, an oscillating sound wave arrives at the input of the 180-degree fold with a uniform pressure p_{in} and volume velocity U_{in}. The total volume velocity U_{in} splits, from the pressure contours it was shown that $U_0 > U_1 > U_2 > U_3 > U_4$. Each individual volume velocity will have a different magnitude and phase as a function of frequency.

At low frequencies, the phases of the individual volume velocities are almost the same. The higher volume velocities at the inner paths effectively shorten the TL producing the higher standing wave frequencies that correlate with the ANSYS FE model results.

At higher frequencies, the differences in the path lengths start to become a bigger fraction of the sound’s wavelength, so magnitude and phase differences exist. The axial standing wave is smeared out over a band of frequencies due to the difference in path lengths, the line’s acoustic impedance and velocity ratio are attenuated in magnitude and spread over a broader frequency range.

For the geometry shown, the maximum path length difference is 23.715” which corresponds to a half wavelength frequency of about 285 Hz. The low pass filtering effect, seen in the right-hand set of plots in the previous slide, starts near this frequency.

Key Take Aways

- I believe that the parallel paths used in the Advance Corner Modeling Method is another step forward in understanding and designing quarter wavelength loudspeaker systems, it is consistent with the FE wave physics in a TL's corner. The number and placement of folds and bends along the TL length can now be used as a design variable to mitigate the higher harmonics and reduce the amount of damping material (meaning more bass output) in the final enclosure.
- The first use of the method was for the referenced Satori TL speaker design, refinements and advances are still being developed. There is much more to explore and learn using this method.
- Additional areas of applicability to be investigate are BLHs, which typically contain many folds, curved path profiles and terminus/mouth shapes that are not consistent with a spherical wave output. The method could probably also be applied to multi-path phase plugs used in compression drivers.
- When I first started exploring TL design methods, over 35 years ago, the focus was exclusively on fiber damping of the standing waves. As I have learned more about TLs, slowly I have shifted my focus to the geometry of the line itself with the damping material becoming much less important in the final design.
- More information about modeling parallel paths is contained in the second and third references.

References

1. Satori Two Year Transmission Line Speaker Design.

http://www.quarter-wave.com/Project13/Project13.html

2. Acoustics of Ducts and Mufflers 2nd Edition by M. L. Munjal, Wiley 2014 (Chapter 4, pages 147 – 150).

3. Passive Damping Mechanism of Herschel-Quincke Tubes for Pressure Pulsations in Piping Systems by Thomas Lato, University of Ontario Masters Degree Thesis.
https://www.researchgate.net/publication/334262904_Passive_Damping_Mechanism_of_Herschel-Quincke_Tubes_for_Pressure_Pulsations_in_Piping_Systems

Attachment 1 : Frequencies and Mode Shapes

The attached ANSYS plots show the quarter-wavelength modes of vibration for the air volume contained in the folded TL geometry. The frequencies are shown in the legends and the color contours present the pressure distribution along the TL's length. The absolute value of the pressure is meaningless since these are all normalized result.

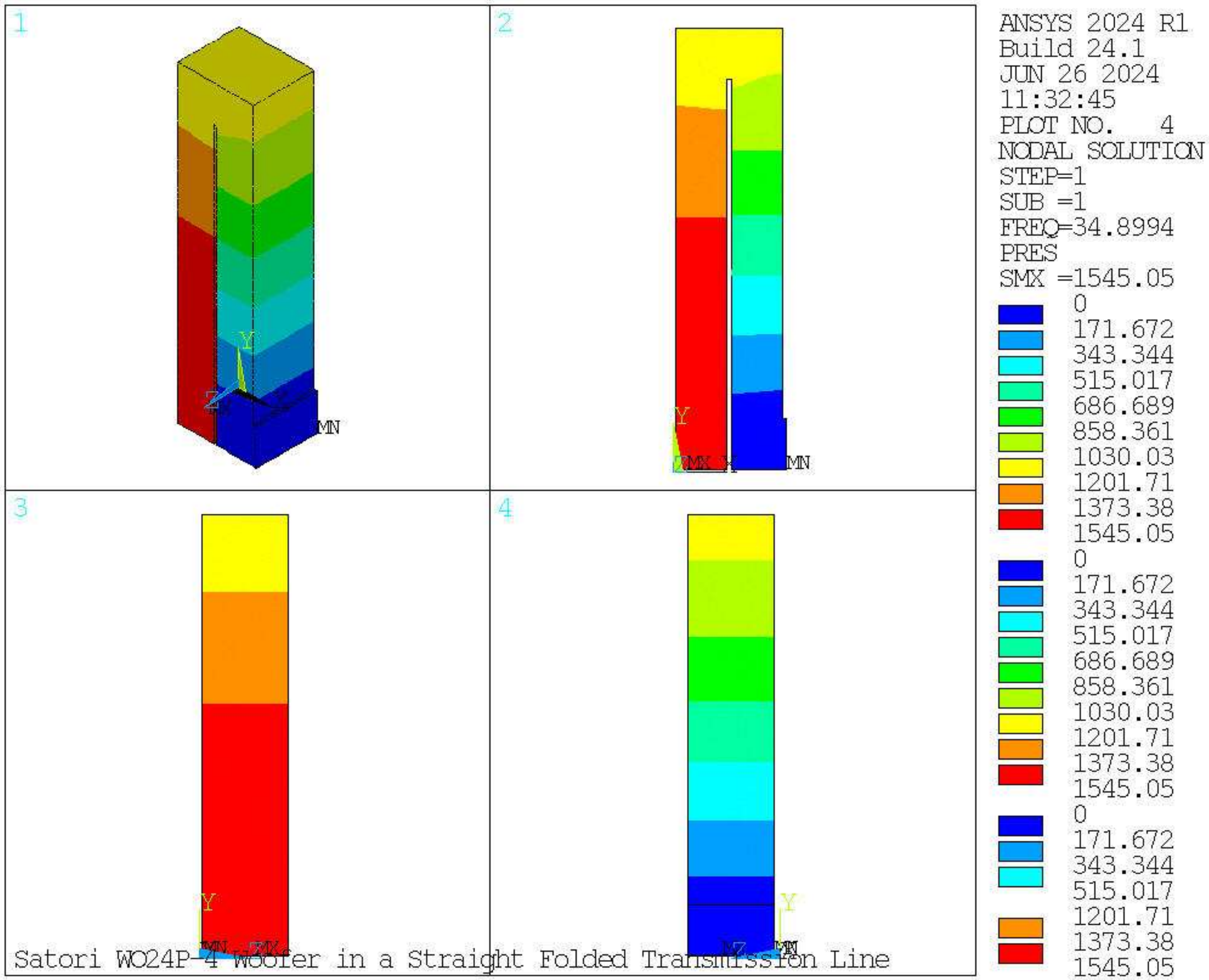

1/4 Wavelength Mode at 34.8994 Hz

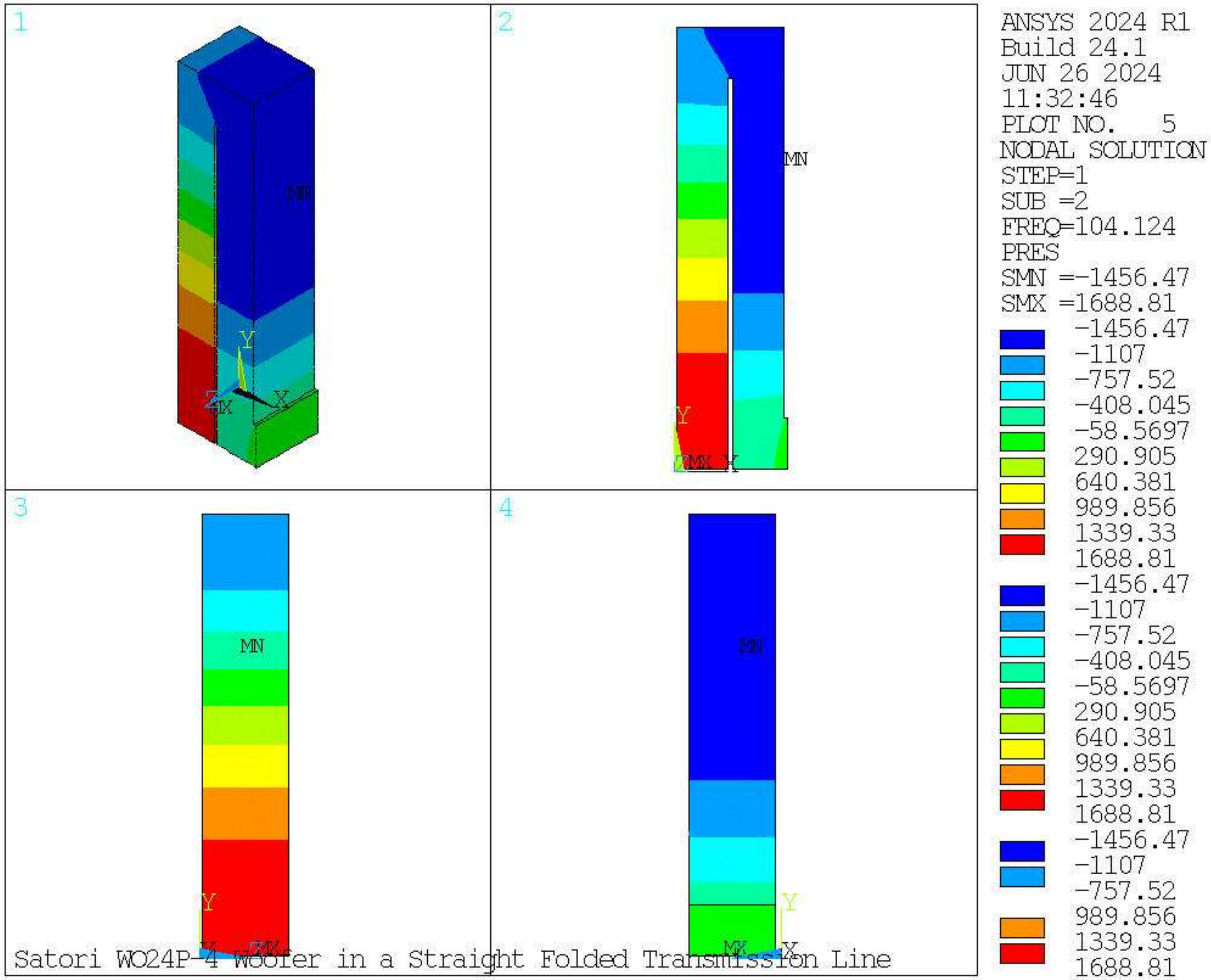

3/4 Wavelength Mode at 104.124 Hz

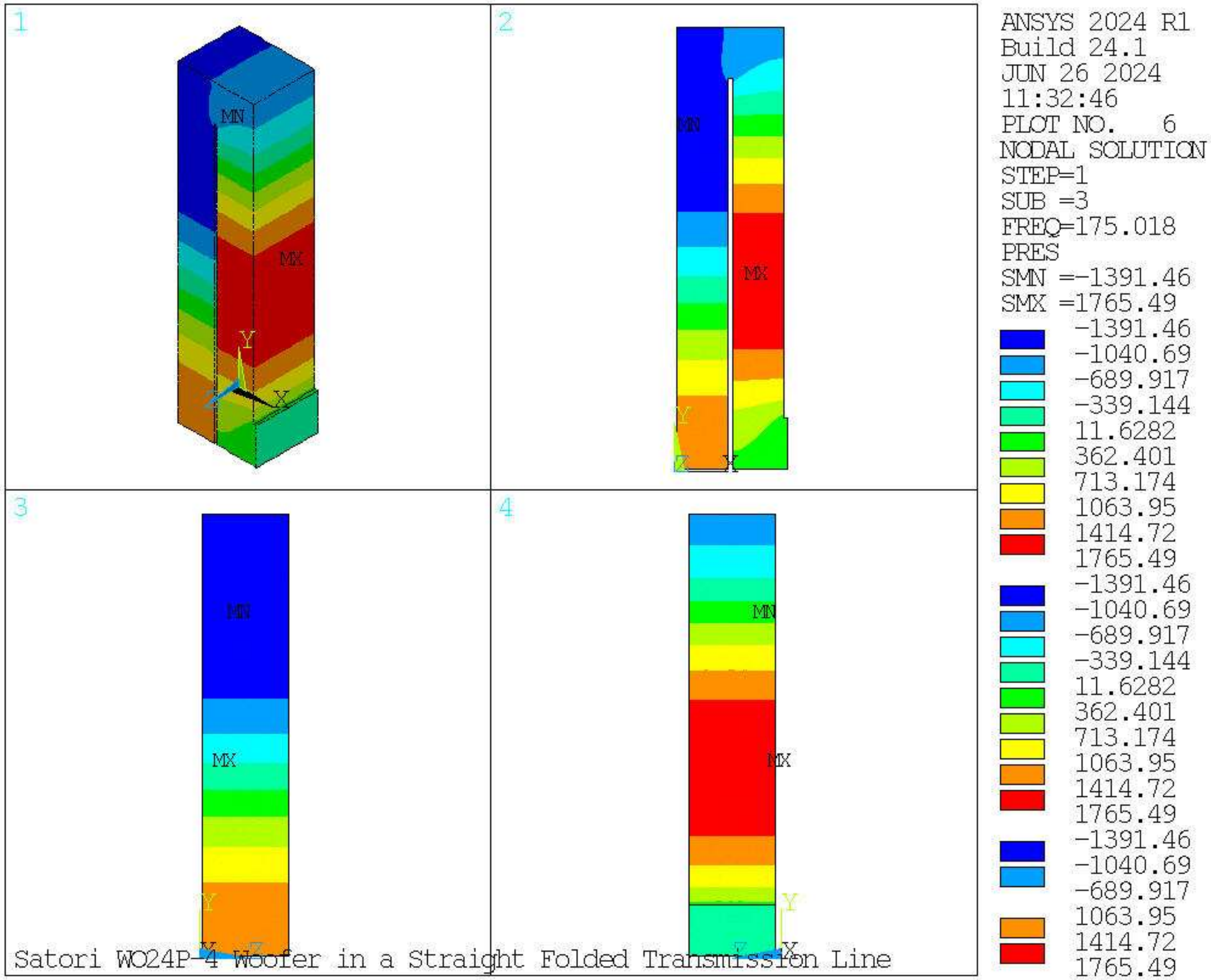

5/4 Wavelength Mode at 175.018 Hz

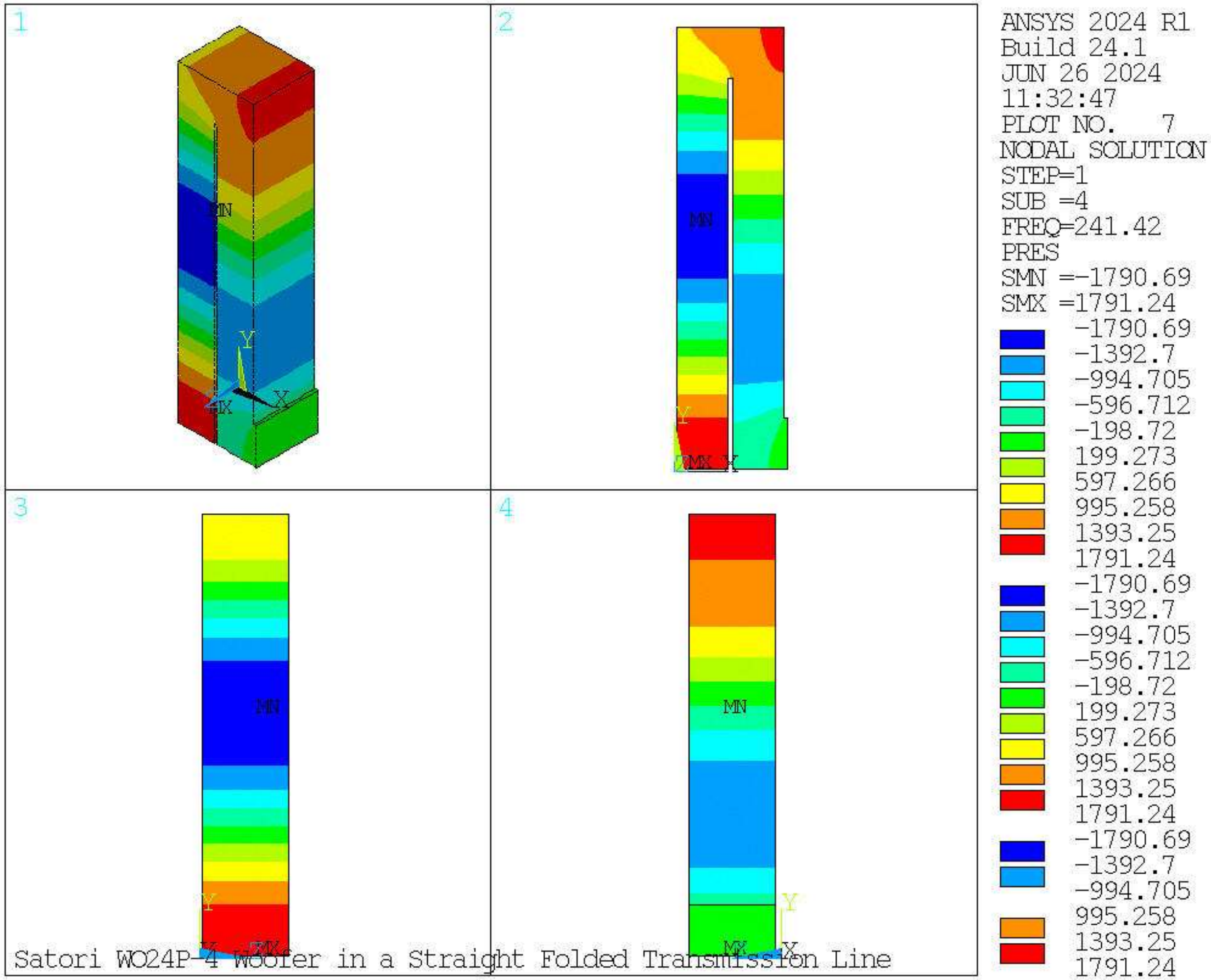

7/4 Wavelength Mode at 241.420Hz

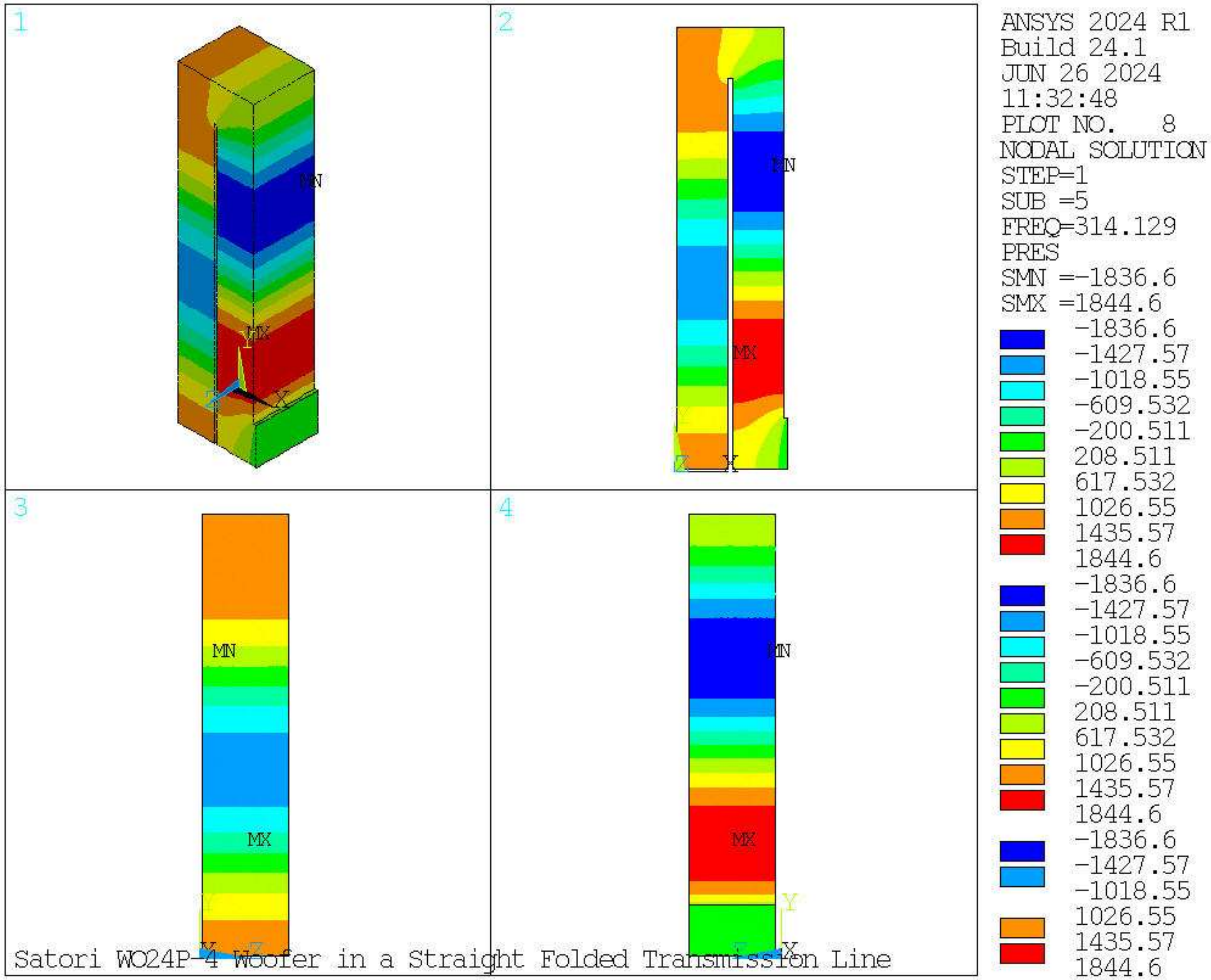

9/4 Wavelength Mode at 314.129 Hz

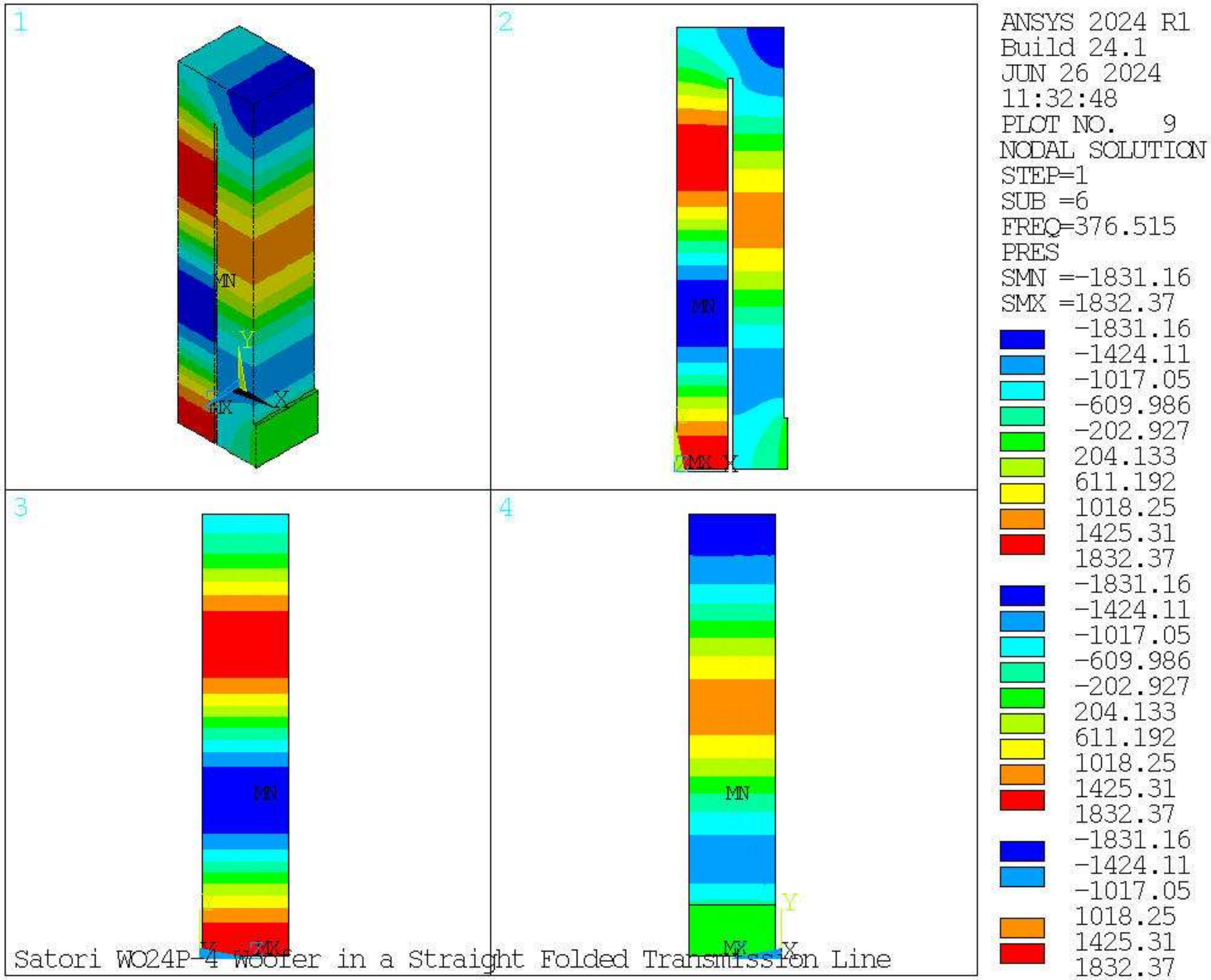

11/4 Wavelength Mode at 376.515 Hz

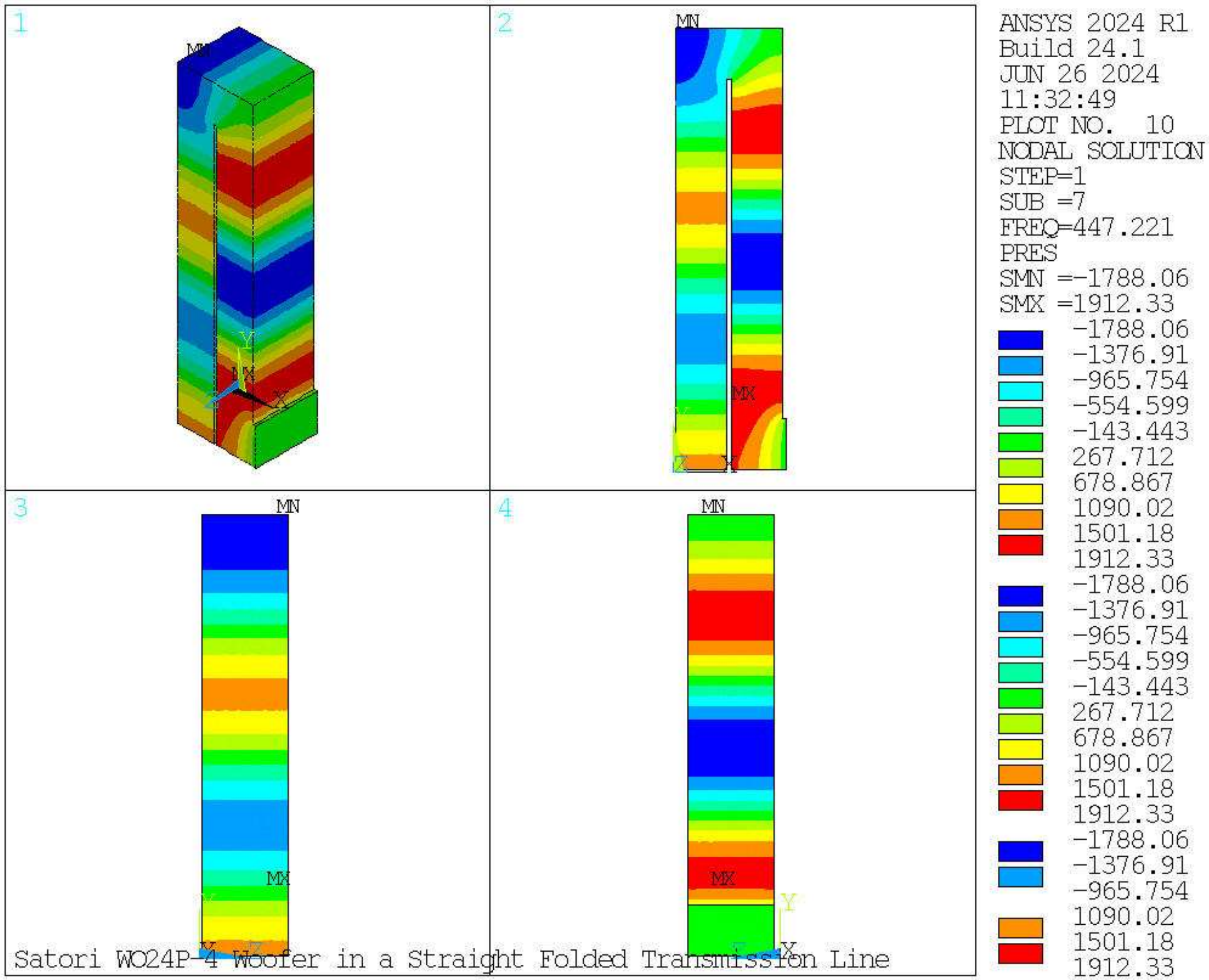

13/4 Wavelength Mode at 447.221 Hz